

2

**INTEGRATED OPTICS ANISOTROPIC
WAVEGUIDES AND DEVICES**

AD-A217 064

FINAL REPORT

Thomas K. Gaylord

April 30, 1989

U. S. ARMY RESEARCH OFFICE

Grant Number: DAAL03-86-K-0157

Georgia Institute of Technology

**DTIC
ELECTE
JAN 22 1990
S B D**

**APPROVED FOR PUBLIC RELEASE;
DISTRIBUTION UNLIMITED.**

90 01 22 134

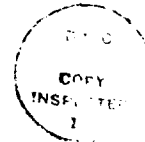
THE VIEW, OPINIONS, AND/OR FINDINGS CONTAINED IN THIS REPORT ARE THOSE OF THE AUTHOR(S) AND SHOULD NOT BE CONSTRUED AS AN OFFICIAL DEPARTMENT OF THE ARMY POSITION, POLICY, OR DECISION, UNLESS SO DESIGNATED BY OTHER DOCUMENTATION.

REPORT DOCUMENTATION PAGE

| | | | |
|--|--|---|-------------------------|
| 1a. REPORT SECURITY CLASSIFICATION Unclassified | | 1b. RESTRICTIVE MARKINGS | |
| 2a. SECURITY CLASSIFICATION AUTHORITY | | 3. DISTRIBUTION/AVAILABILITY OF REPORT Approved for public release; distribution unlimited. | |
| 2b. DECLASSIFICATION/DOWNGRADING SCHEDULE | | 4. PERFORMING ORGANIZATION REPORT NUMBER(S) | |
| 4. PERFORMING ORGANIZATION REPORT NUMBER(S) | | 5. MONITORING ORGANIZATION REPORT NUMBER(S) ARO 23602.2-EL | |
| 6a. NAME OF PERFORMING ORGANIZATION School of Electrical Engr. Georgia Institute of Technology | 6b. OFFICE SYMBOL (if applicable) | 7a. NAME OF MONITORING ORGANIZATION U. S. Army Research Office | |
| 6c. ADDRESS (City, State, and ZIP Code) Atlanta, Georgia 30332 - 0250 | | 7b. ADDRESS (City, State, and ZIP Code) P. O. Box 12211 Research Triangle Park, NC 27709-2211 | |
| 8a. NAME OF FUNDING/SPONSORING ORGANIZATION U. S. Army Research Office | 8b. OFFICE SYMBOL (if applicable) | 9. PROCUREMENT INSTRUMENT IDENTIFICATION NUMBER DAAL03-86-K-0157 | |
| 8c. ADDRESS (City, State, and ZIP Code) P. O. Box 12211 Research Triangle Park, NC 27709-2211 | | 10. SOURCE OF FUNDING NUMBERS | |
| | | PROGRAM ELEMENT NO. | PROJECT NO. |
| | | TASK NO. | WORK UNIT ACCESSION NO. |
| 11. TITLE (Include Security Classification) Integrated Optics Anisotropic Waveguides and Devices | | | |
| 12. PERSONAL AUTHOR(S) Thomas K. Gaylord | | | |
| 13a. TYPE OF REPORT Final | 13b. TIME COVERED FROM <u>8-86</u> TO <u>4-89</u> | 14. DATE OF REPORT (Year, Month, Day) 1989 April 30 | 15. PAGE COUNT 48 |
| 16. SUPPLEMENTARY NOTATION The view, opinions and/or findings contained in this report are those of the author(s) and should not be construed as an official Department of the Army position, policy, or decision, unless so designated by other documentation. | | | |
| 17. COSATI CODES | | 18. SUBJECT TERMS (Continue on reverse if necessary and identify by block number) | |
| FIELD | GROUP | SUB-GROUP | |
| | | integrated optics, birefringence, gyrotropic, electro-optic | |
| 19. ABSTRACT (Continue on reverse if necessary and identify by block number) | | | |
| <p>Many practical modulator materials include combinations of electro-optically induced birefringence, optical activity, and/or Faraday rotation. Thus, there is a need for a procedure to design and analyze devices fabricated with materials exhibiting any or all of these effects. In this final report a simple procedure employing an extension of the general Jacobi method is introduced for determining the properties of the two allowed elliptical eigen-polarizations for an arbitrary direction of propagation as well as the principal indices and axes of a general lossless, electro-optic, and gyrotropic medium. The Jacobi method presented in this work is an</p> | | | |
| 20. DISTRIBUTION/AVAILABILITY OF ABSTRACT <input type="checkbox"/> UNCLASSIFIED/UNLIMITED <input type="checkbox"/> SAME AS RPT. <input type="checkbox"/> DTIC USERS | | 21. ABSTRACT SECURITY CLASSIFICATION Unclassified | |
| 22a. NAME OF RESPONSIBLE INDIVIDUAL | | 22b. TELEPHONE (Include Area Code) | 22c. OFFICE SYMBOL |

19. ABSTRACT (continued)

iterative procedure used for performing a unitary transformation to diagonalize the Hermitian impermeability tensor. In addition, a complex polarization variable is defined from elements of the unitary transformation matrix to determine the ellipticity, azimuth angle, relative amplitude and phase, and handedness of the two orthogonal elliptical polarizations. Also, the phase velocity indices of refraction are readily calculated with simple derived expressions. This procedure is numerically stable and accurate for any crystal, external field direction, and direction of propagation.



| | |
|----------------------|-------------------------------------|
| Accession For | |
| NTIS GRA&I | <input checked="" type="checkbox"/> |
| DTIC TAB | <input type="checkbox"/> |
| Unannounced | <input type="checkbox"/> |
| Justification | |
| By _____ | |
| Distribution/ | |
| Availability Codes | |
| Dist | Avail and/or Special |
| A-1 | |

I. Introduction

In a recent publication,¹ a straightforward, numerically stable method for performing electro-optic effect calculations was presented. Simple analytic procedures were developed for calculating the principal dielectric axes and refractive indices of an electro-optic crystal of any crystal class subject to an external electric field applied in a general direction. Simple formulas were also developed for obtaining the two allowed eigen-polarizations and their corresponding refractive indices for a general direction of phase propagation. However, in addition to an external electric field, the optical properties of a crystal may be affected by other influences, internal or external, such as natural optical activity, an internal or applied magnetic field, stress, and others. The optical properties and the induced changes in them may be described by the relative permittivity tensor $[\epsilon]$ or its inverse, the impermeability tensor $[\eta]$, where $[\eta] = [\epsilon]^{-1} = [1/n^2]$ and n is the index of refraction.

The linear and quadratic electro-optic effects induce changes in the linear birefringence of a crystal. These effects may be represented as symmetric perturbations to the impermeability tensor. The allowed polarizations remain linear, regardless of the direction of propagation. However, some electro-optic crystals such as bismuth silicon oxide are also optically active, thereby exhibiting natural reciprocal circular birefringence. This physical effect is manifested as a rotation of the linear polarization of the light upon transmission through the crystal. Correspondingly, the eigen-polarizations are no longer linear but are, in general, elliptical. Rotation of linearly polarized light may also be induced by an external field. For example, an applied magnetic field may induce nonreciprocal circular birefringence (Faraday rotation).

Furthermore, an external electric field may induce reciprocal circular birefringence (electrogyration effect). Media exhibiting circular birefringence, whether natural or induced, are referred to as *gyrotropic*. The mechanisms giving rise to gyrotropy may be represented as imaginary antisymmetric (Hermitian) perturbations to the impermeability tensor.

The two general questions to be addressed here are as follows: 1) Given a crystal that is linear birefringent (natural or induced) and/or gyrotropic (natural or induced), what are the principal refractive indices and principal dielectric axes of the crystal? 2) What are the two eigenstates (i.e., phase velocity indices and corresponding eigen-polarizations) for a given direction of light propagation? The other given conditions are that the crystal is lossless, linear, and homogeneous. The answers to the above questions can be obtained by first determining the eigenvalues and eigenvectors of the perturbed impermeability tensor. In addition, since the eigen-polarizations are now elliptical in general, three pieces of information are required to describe each state of polarization: azimuth angle, ellipticity, and handedness.

Similar problems with the electromagnetic description of gyrotropy have been addressed in the literature in terms of macroscopic theory²⁻⁹ and quantum mechanics.⁹⁻¹¹ As an example of the former, a method to calculate the eigenstates of a naturally optically active, electro-optic crystal by diagonalizing the coupled-wave equations was presented by Yariv and Lotspeich.³ As an example of the latter, a method using quantum electrodynamics to determine the eigenstates in optically active, linear birefringent crystals was presented by Eimerl.¹⁰ The approach presented in this paper is based on the macroscopic properties of the crystal. The procedure introduced here employs an extension of the general Jacobi method, a known, very accurate, stable, and simple numerical routine. Also, to

obtain a full description of the eigen-polarizations, a complex polarization variable is used that maps the eigenvectors of the transverse impermeability tensor into a complex polarization plane. The advantages of this method over the others are that (1) no assumptions are required; (2) it applies to any crystal class; (3) it applies to any field direction; (4) it applies to any direction of light propagation; and (5) it is numerically stable, accurate, and straightforward.

The constitutive equation will first be used to describe the optical properties of a crystal. To provide a geometric interpretation of linear and circular birefringence, the index ellipsoid and gyration surface will be reviewed. Next, the procedure to address the given problem will be introduced, which includes a brief overview of the eigenvalue/eigenvector problem for Hermitian matrices, followed by a description of the extended Jacobi method introduced in the present work and of the complex polarization variable used to obtain the eigenstates for a given direction of phase propagation. Finally, bismuth silicon oxide, an optically active, electro-optic, electrogyratory material is analyzed to illustrate the simplicity and accuracy of the method. Throughout this paper boldface will be used to denote a vector and $[\cdot]$ to denote a matrix.

II. Constitutive Equation

The material properties (principal permittivities or refractive indices) of the crystal are represented by the constitutive relation $\mathbf{D} = [\epsilon]\mathbf{E}$, where $[\epsilon]$ is the permittivity tensor of the medium. Disturbances to the optical properties, which are typically very small in magnitude, may be described by this tensor. They are commonly expressed in terms of the inverse of the permittivity tensor, $[\epsilon]^{-1} = 1/\epsilon_0 [\epsilon]^{-1} = 1/\epsilon_0 [1/n^2]$, where ϵ_0 is the permittivity of free space.

For a homogeneous, lossless, and nongyrotropic medium the permittivity (impermeability) tensor has only real components. Moreover, it is symmetric for all crystal classes and for any selection of the dielectric axes.¹²⁻¹⁴ Therefore, it may be diagonalized, and in principal coordinates, the constitutive equation is

$$\begin{bmatrix} D_x \\ D_y \\ D_z \end{bmatrix} = \begin{bmatrix} \epsilon_x & 0 & 0 \\ 0 & \epsilon_y & 0 \\ 0 & 0 & \epsilon_z \end{bmatrix} \begin{bmatrix} E_x \\ E_y \\ E_z \end{bmatrix}, \quad (1)$$

with the principal permittivities on the diagonal. The symmetry of $[\epsilon]$ guarantees that a diagonal form exists given a correct choice of three perpendicular principal axes (x,y,z) with respect to the crystallographic axes.

If the medium is gyrotropic, the constitutive equation may be written as¹³⁻¹⁵

$$D = [\epsilon]E + i\epsilon_0 G \times E = [\epsilon]'E, \quad (2)$$

where $[\epsilon]$ is the symmetric unperturbed permittivity tensor, i is $\sqrt{-1}$, and G is the gyration vector which is uniquely defined for the mechanism producing the circular birefringence. The vector cross product $G \times E$ in Eq. (2) may be represented as the product of an antisymmetric tensor $[G]$ with the vector E . Thus,

$$D = ([\epsilon] + i\epsilon_0 [G])E = [\epsilon]'E. \quad (3)$$

Therefore, the permittivity tensor $[\epsilon]'$ is now clearly Hermitian as indeed it must be due to thermodynamic arguments.¹³⁻¹⁴

The constitutive equation may also be written as

$$E = [\epsilon]'^{-1}D = [\eta]'D = (1/\epsilon_0)([\eta] - i[\eta][G][\eta])D. \quad (4)$$

From Eq. (4), the antisymmetric (imaginary) part of $[\eta]'$ is

$$\text{Im}[\eta]' = -[\eta][G][\eta] = - \begin{bmatrix} 0 & -\eta_x \eta_y G_z & \eta_x \eta_z G_y \\ \eta_x \eta_y G_z & 0 & -\eta_y \eta_z G_x \\ -\eta_x \eta_z G_y & \eta_y \eta_z G_x & 0 \end{bmatrix}. \quad (5)$$

An important point is that the imaginary part of $[\eta]'$ has no effect on the principal dielectric axes and indices of the crystal. The real part of $[\eta]'$ is real and symmetric.

A number of the various types of influences, both natural and induced, on the optical properties are now described.

A. Dielectric Properties with No Fields Applied

1. Natural Linear Birefringence

The optical symmetry of a crystal is represented by the permittivity (impermeability) tensor.¹²⁻¹⁴ If all diagonal elements are equal, then the crystal is isotropic. If $\epsilon_x = \epsilon_y \neq \epsilon_z$, then the crystal is uniaxial. If $\epsilon_x \neq \epsilon_y \neq \epsilon_z \neq \epsilon_x$, the crystal is biaxial. Therefore, both uniaxial and biaxial crystals exhibit natural linear birefringence; e.g., $\epsilon_z - \epsilon_y \neq 0$.

2. Natural Optical Activity

In general, the macroscopic properties of a medium depend on the temporal and/or spatial variation of the electromagnetic field. For the case of natural optical activity, the properties are influenced by spatial dispersion, the dependence of $[\epsilon]$ on the magnitude and direction of k at fixed frequency.^{4, 13-19} The macroscopic dipole moment per unit volume of the medium at a given point depends on the field at and near that point. In the optical frequency range, the effects of spatial dispersion, in general, are small and are characterized by the first power of a/λ ($\ll 1$), where a is on the order of the lattice constant and λ is the wavelength of the light in

the medium. Therefore, to first order, the constitutive equation is^{14-15,17-18}

$$D_i = \epsilon_{ij} E_j + \gamma_{ijl} (\partial E_j / \partial x_l) = \epsilon'_{ij} E_j \quad (6)$$

and

$$\epsilon'_{ij} = \epsilon'_{ij}(\omega, \mathbf{k}) = \epsilon_{ij}(\omega) + i\gamma_{ijl}(\omega) k_l, \quad (7)$$

where $\epsilon_{ij}(\omega)$ is the permittivity tensor without optical activity and $\gamma_{ijl}(\omega)$ is a third-rank real antisymmetric tensor in the indices i and j , resulting in ϵ'_{ij} being Hermitian. The second term can also be represented by $\mathbf{G} \times \mathbf{E}$, where \mathbf{G} is the gyration (axial) vector.¹³⁻¹⁵

The displacement vector \mathbf{D} rotates in a helical fashion about the wavevector \mathbf{k} , so \mathbf{G} is parallel to \mathbf{k} and the components of \mathbf{G} are functions of the direction cosines of \mathbf{k} . The sense of rotation bears a fixed relation to the direction of propagation as shown in Fig. 1a. If a linearly polarized input light wave is transmitted through an optically active crystal and then is reflected back through the crystal, the net rotation of the polarization is zero. Therefore, natural optical activity is a reciprocal effect.^{4,13}

By defining the direction of \mathbf{k} in spherical coordinates (ϕ_k, θ_k) , the components and magnitude of \mathbf{G} are^{13,17}

$$\begin{aligned} G_x &= G \sin \theta_k \cos \phi_k, & G_y &= G \sin \theta_k \sin \phi_k, & G_z &= G \cos \theta_k \\ |G| &= G = g_{11} \sin^2 \theta_k \cos^2 \phi_k + g_{22} \sin^2 \theta_k \sin^2 \phi_k + g_{33} \cos^2 \theta_k \\ &\quad + 2g_{12} \sin^2 \theta_k \sin \phi_k \cos \phi_k + 2g_{13} \sin \theta_k \cos \theta_k \cos \phi_k \\ &\quad + 2g_{23} \sin \theta_k \cos \theta_k \sin \phi_k, \end{aligned} \quad (8)$$

where g_{ij} are the components of the gyration tensor. Only noncentrosymmetric crystals can have natural optical activity. Table I provides a summary of the gyration tensors for all crystal classes that exhibit optical activity.¹³

B. Dielectric Properties with External Fields Applied

1. Linear Electro-Optic Effect

An electric field applied in an arbitrary direction to a crystal lacking a center of symmetry produces a change in the coefficients $(1/n^2)_i$ due to the linear electro-optic effect according to

$$\Delta(1/n^2)_i = \sum_j r_{ij} E_j \quad \begin{array}{l} i = 1, \dots, 6 \\ j = x, y, z = 1, 2, 3 \end{array} \quad (9)$$

where r_{ij} is the ij^{th} element of the linear electro-optic tensor in reduced-subscript notation.^{13, 20} In matrix form Eq. (9) is

$$\begin{bmatrix} \Delta(1/n^2)_1 \\ \Delta(1/n^2)_2 \\ \Delta(1/n^2)_3 \\ \Delta(1/n^2)_4 \\ \Delta(1/n^2)_5 \\ \Delta(1/n^2)_6 \end{bmatrix} = \begin{bmatrix} r_{11} & r_{12} & r_{13} \\ r_{21} & r_{22} & r_{23} \\ r_{31} & r_{32} & r_{33} \\ r_{41} & r_{42} & r_{43} \\ r_{51} & r_{52} & r_{53} \\ r_{61} & r_{62} & r_{63} \end{bmatrix} \begin{bmatrix} E_x \\ E_y \\ E_z \end{bmatrix}. \quad (10)$$

For a noncentrosymmetric crystal, the new impermeability tensor in the presence of an applied electric field is, in general, no longer diagonal in the original axes system. The perturbed impermeability tensor is

$$[1/n^2]' = \begin{bmatrix} 1/n_1^2 + \Delta(1/n^2)_1 & \Delta(1/n^2)_6 & \Delta(1/n^2)_5 \\ \Delta(1/n^2)_6 & 1/n_2^2 + \Delta(1/n^2)_2 & \Delta(1/n^2)_4 \\ \Delta(1/n^2)_5 & \Delta(1/n^2)_4 & 1/n_3^2 + \Delta(1/n^2)_3 \end{bmatrix}. \quad (11)$$

However, the field-induced perturbations are real and symmetric, so the symmetry of the tensor is not disturbed. These changes to $[1/n^2]$ have the effect of changing the principal axes and indices of the crystal. The electro-optic tensor for all crystal classes is summarized in numerous texts.^{13, 15} All optically active crystals are also electro-optic, but the converse is not true.

2. Electrogyration Effect

An applied electric field may not only induce linear birefringence, but in many cases,²¹ it may also induce circular birefringence through the electrogyration (EG) effect. Considering only first-order spatial dispersion, the gyration tensor is²¹⁻²³

$$g_{ij}' = g_{ij} + \mu_{ijk} E_k, \quad (12)$$

where g_{ij} is the gyration tensor with no applied field and μ_{ijk} is the third-rank electrogyration tensor, which has the same symmetry as the electro-optic tensor. The second-rank tensor $\mu_{ijk} E_k$ alters g_{ij} in the same manner as Eq. (9) alters the impermeability tensor in Eq. (11). The net result is a change in the magnitude of the gyration vector G as found by Eq. (8) and therefore, a change in the specific rotation (polarization rotation per unit thickness) of the medium. The EG effect may be viewed as induced optical activity, a reciprocal effect. This perturbation changes the impermeability tensor in the same manner as optical activity, that is, producing Hermitian off-diagonal elements as in Eq. (4) rather than the real symmetric off-diagonal elements of Eq. (11).

3. Faraday Rotation

In a Faraday active medium, the macroscopic properties are influenced by frequency dispersion caused by an applied magnetic field.^{4, 8, 13-14, 24-27} The field creates a relative shift between the phase velocity indices of refraction of the two allowed eigen-polarizations, inducing circular birefringence. The constitutive equation is

$$D = [\epsilon]E + i\epsilon_0\psi B \times E, \quad (13)$$

where $[\epsilon]$ is the unperturbed permittivity tensor and ψ is the

magnetogyration constant of the medium. The real part of the impermeability tensor is symmetric in B , and the imaginary part is antisymmetric in B .¹⁴ Since only first-order effects are considered, the real part of the tensor remains unchanged. In this case, the imaginary part is represented by the gyration vector that is proportional to B ; i.e., $G = \psi B$. Thus, the components of G are functions of the direction cosines of B (ϕ_B, θ_B), rather than those of k . That is,

$$G_x = \psi B \sin \theta_B \cos \phi_B, \quad G_y = \psi B \sin \theta_B \sin \phi_B, \quad G_z = \psi B \cos \theta_B. \quad (14)$$

The magnitude of G is merely the product of ψ and the magnitude of B . For Faraday rotation, the sense of rotation bears a fixed relation to B , as shown in Fig. 1b. The eigen-polarizations are preserved upon reflection so that the net rotation is doubled. Thus, Faraday rotation is a nonreciprocal effect.^{4, 11, 13}

C. Combined Effects

If, for example, a lossless, biaxial, and optically active crystal is subject to an applied electric field, then the impermeability tensor is altered by Hermitian perturbations and is^{5, 13-14, 24}

$$[1/n^2]' = [\eta]' = \begin{bmatrix} \eta_{xx} & \eta_{xy} & \eta_{xz} \\ \eta_{xy}^* & \eta_{yy} & \eta_{yz} \\ \eta_{xz}^* & \eta_{yz}^* & \eta_{zz} \end{bmatrix}, \quad (15)$$

where η_{ij} , $i \neq j$, are complex and η_{ii} are real. As stated previously, the imaginary parts of the off-diagonal elements do not affect the principal axes or indices of the crystal. They affect only the state of the allowed polarizations and the phase velocity indices. The eigen-polarizations are now elliptical, in general, rather than linear as with the electro-optic effect. An Hermitian matrix may be represented by a quadratic surface in

complex space. In real Cartesian space, however, only the real part of $[\eta]'$, which is symmetric, contributes to a quadratic surface (ellipsoid). Geometric surfaces which represent optical properties of the crystal are discussed in the next section.

III. Geometric Approach

A. Index Ellipsoid

The index ellipsoid is a construct whose geometric characteristics represent the phase velocities and the directions of electric displacement vibration of the two allowed plane waves corresponding to a given optical wavevector direction in a crystal. The general index ellipsoid for an optically biaxial crystal is expressed in Cartesian coordinates as¹²⁻¹³

$$\left(\frac{x^2}{n_x^2}\right) + \left(\frac{y^2}{n_y^2}\right) + \left(\frac{z^2}{n_z^2}\right) = 1 \quad (16)$$

where n_x , n_y , and n_z are the principal refractive indices of the crystal. Since the permittivity (impermeability) tensor is positive definite, the surface is always an ellipsoid. If $n_x = n_y$, the surface becomes an ellipsoid of revolution, representing a uniaxial crystal. An isotropic crystal is represented by a sphere (degenerate ellipsoid) with the principal axes having equal length. These surfaces are shown in Fig. 1 of Ref. 1. Also, shown are the optic axes for each crystal symmetry.

The eigenstates for an arbitrary direction of propagation in a crystal are found in the elliptical cross-section perpendicular to \mathbf{k} which passes through the origin of the index ellipsoid, as shown in Fig. 2. If the optical properties are not disturbed, the major and minor axes of the cross-section ellipse represent the two allowed orthogonal linear vibration directions of \mathbf{D} (eigen-polarizations) for that particular direction of propagation. The lengths of these axes correspond to the the respective

phase velocity indices of the allowed polarizations. They are, therefore, referred to as the "fast" and "slow" axes. As with the principal axes and indices of the crystal, these eigenstates, in general, are affected by real symmetric perturbations, (for example, the electro-optic effect), to the impermeability tensor. However, the antisymmetric perturbations affect only the eigenstates (the eigen-polarizations and phase velocity indices). The major axes of the cross-section ellipse correspond to the major axes of the allowed polarizations in this case.

B. Gyration Surface

The geometry of the index ellipsoid provides only partial information about the eigenstates if the allowed polarizations are not linear. In this case the ellipsoid can be used to determine only the orientation of the allowed elliptical polarizations but nothing on the properties of optical rotation for a given wavevector direction. The gyration surface, however, may be used to illustrate the directional dependence of optical rotation in a gyrotropic crystal. For optically active crystals the surface is constructed from the gyration tensor $[g]$ in the same way that the index ellipsoid is constructed from the impermeability tensor.¹⁷ That is, the distance from the origin to any point on the surface is given by

$$G = g_{ij} k_i k_j, \quad (17)$$

where k_i and k_j are the direction cosines of the wavevector k . Equation (17) is the directional magnitude of the gyration vector, $G = |G|$, as given by Eq. (8). Since the gyration tensor is not necessarily positive definite, the surface may have a variety of forms. Shubnikov¹⁷ provides a complete set of all possible surfaces for isotropic, uniaxial, and biaxial crystal classes which exhibit optical activity. For example, Fig. 3 is the gyration

surface for right-handed quartz (class 32) which is positive uniaxial and optically active. The first two diagonal elements, $\epsilon_{11} = \epsilon_{22}$, are negative, and ϵ_{33} is positive. The surface is given by $G = -|\epsilon_{11}| \sin^2 \theta_{k_0} + \epsilon_{33} \cos^2 \theta_{k_0}$, where θ_{k_0} is the angle between the optic axis and \mathbf{k} . Therefore, optical rotation along the optic axis is right-handed and is denoted by the white surface. However, propagation perpendicular to the optic axis gives optical rotation in the opposite direction and is denoted by the dark surface. There is no optical rotation ($G = 0$) for propagation directed -56° from the optic axis, as determined by the measured quantity $\epsilon_{11}/\epsilon_{33} \sim 0.45$, and the eigen-polarizations are linear.

For Faraday active crystals a gyration surface may also be constructed. As stated before, the sense of optical rotation bears a fixed relation to the direction of the applied magnetic field \mathbf{B} . Maximum rotation is achieved for propagation parallel and antiparallel to the applied magnetic field. If propagation is in a direction inclined to \mathbf{B} , the degree of optical rotation will decrease as $\cos \theta_{\mathbf{kB}}$, where $\theta_{\mathbf{kB}}$ is the angle between \mathbf{k} and \mathbf{B} .¹⁴ Therefore, Fig. 4 is a representation of the gyration surface for this type of crystal.

IV. Analysis

The problem is to determine the principal axes and indices of the crystal and the two allowed orthogonal eigenstates of polarization (D_1 and D_2) and the corresponding phase velocity indices (n_1 and n_2) for a general wavevector direction and a general external field. The solution to the problem lies in determining the eigenvalues and eigenvectors of Eq. (15). The method chosen to address this problem involves diagonalizing the matrix using an extension of the general Jacobi method. For Hermitian matrices, the eigenvalues are real. The eigenvectors, on the other hand, are complex

in general. Thus, additional information is required to describe the general state of the eigen-polarizations (the complex eigenvectors). For linear polarization, only the orientation (azimuth angle) in the plane transverse to \mathbf{k} is required. For elliptical polarization, the ellipticity and handedness as well as the azimuth angle must be determined. Furthermore, for linear polarization, D oscillates in a plane in one fixed direction perpendicular to \mathbf{k} . If D is elliptically polarized, then it no longer oscillates in a plane but rather propagates in a flattened helix about \mathbf{k} , as shown in Fig. 5. A full description of the eigen-polarizations is obtained by using a complex polarization variable.

A. Principal Axes and Principal Refractive Indices

A detailed description of a procedure to determine the new principal axes and indices of a crystal subject to real symmetric perturbations is given in Ref. 1. That approach employs the general Jacobi method, and it is known to be an accurate, numerically stable, and simple routine for diagonalizing real symmetric matrices. The routine is iterative, and it involves the calculation of an elementary plane rotation angle at each step to zero the largest off-diagonal element. Also, the method allows for consistent labeling of the new axes; a global rotation axis and a global rotation angle are calculated from the resulting cumulative orthogonal transformation matrix. To find the principal axes and indices of a crystal with Hermitian perturbations to its optical properties, as given by Eq. (15), the same procedure is performed but only on the real part of the matrix. The authors refer the reader to Ref. 1 for this part of the analysis.

B. Eigenstates of Polarization and Phase Velocity Indices

The eigenvalue problem for Hermitian matrices is addressed by a unitary

transformation, $[a][\eta]'[a]^H = [\lambda]$, where $[a]$ is the unitary transformation matrix ($[a]^H = [a]^{-1}$), $[\eta]'$ is an Hermitian matrix, $[\lambda]$ is the resulting diagonal matrix of real eigenvalues, and H denotes complex conjugate transpose. As suggested by Wilkinson,²⁸ a form of the unitary matrix that can be used is

$$[a] = \begin{bmatrix} \cos\Phi & e^{iB}\sin\Phi \\ -e^{-iB}\sin\Phi & \cos\Phi \end{bmatrix}. \quad (18)$$

This matrix has the effect of transforming a system from Cartesian coordinates to a complex (helical) coordinate system.²⁹ There are two parameters, Φ and B , to determine. For real symmetric matrices $B = 0$, and Φ represents the elementary Cartesian plane rotation angle. Using the expression for a unitary transformation, a set of relationships was derived (with the unitary matrix of Eq. (18)), which results in a version of the general Jacobi method extended to Hermitian matrices. The two unknowns Φ and B are calculated at each iteration step. With additional algebra, the simple expressions in the Appendix were obtained for updating the elements of $[\eta]'$ as the diagonalization process proceeds. The parameter B was determined to be the argument of the off-diagonal element η_{ij} , $i \neq j$, and is the required value for zeroing that element with a rotation in the (i,j) complex plane. These formulas reduce to those of the general Jacobi method for real symmetric matrices.¹ The Jacobi method using these modified formulas was programmed and tested. The results for several test matrices were found with virtually zero error. These results were often more accurate than those obtained with the commercial IMSL³⁰ routine, EIGCH.

To find the eigenstates for a specific direction of propagation k , a real orthogonal transformation must first be performed on the Hermitian matrix $[\eta]'$ to place the problem in a coordinate system of k . The

wavevector direction is specified by the spherical coordinates (ϕ_k, θ_k) in the original (x, y, z) coordinate system. A new coordinate system (x'', y'', z'') is defined with z'' parallel to k and x'' lying in the (z, z'') plane. The transformation to the (x'', y'', z'') system is produced first by a rotation ϕ_k about the z -axis followed by a rotation θ_k about y'' as shown in Fig. 6. This transformation is described by

$$\begin{aligned} x'' &= x \cos\theta_k \cos\phi_k + y \cos\theta_k \sin\phi_k - z \sin\theta_k \\ y'' &= -x \sin\phi_k + y \cos\phi_k \\ z'' &= x \sin\theta_k \cos\phi_k + y \sin\theta_k \sin\phi_k + z \cos\theta_k. \end{aligned} \quad (19)$$

The transformed tensor $[\eta]''$ in the (x'', y'') plane is

$$[\eta]'' = \begin{bmatrix} \eta_{xx}'' & \eta_{xy}'' \\ \eta_{xy}^{*''} & \eta_{yy}'' \end{bmatrix}, \quad (20)$$

where

$$\begin{aligned} \eta_{xx}'' &= (\eta_{xx} \cos^2\phi_k + \eta_{yy} \sin^2\phi_k) \cos^2\theta_k + \eta_{zz} \sin^2\theta_k + \\ &\quad 2\eta_{xyr} \cos^2\theta_k \cos\phi_k \sin\phi_k - 2\cos\theta_k \sin\theta_k (\eta_{xzz} \cos\phi_k + \eta_{yzz} \sin\phi_k), \\ \eta_{yy}'' &= \eta_{xx} \sin^2\phi_k + \eta_{yy} \cos^2\phi_k - 2\eta_{xyr} \cos\phi_k \sin\phi_k, \\ \eta_{xy}'' &= (\eta_{yy} - \eta_{xx}) \cos\theta_k \cos\phi_k \sin\phi_k + \cos\theta_k (\eta_{xy} \cos^2\phi_k - \eta_{xy}^* \sin^2\phi_k) \\ &\quad + \sin\theta_k (\eta_{xz}^* \sin\phi_k - \eta_{yz}^* \cos\phi_k) - \eta_{yx}^{*''}, \end{aligned} \quad (21)$$

and η_{ijr} denotes the real part of η_{ij} . Therefore, the Hermitian property is preserved. The third row and column can be neglected, since the vibration direction of the eigen-polarizations is transverse to k . Next, the phase velocity indices of refraction are easily determined using the relationships in the Appendix (with a slight modification) to diagonalize the 2×2 matrix of Eq. (20). The required rotation in the complex (x'', y'') plane is

$$\Phi = \frac{1}{2} \tan^{-1} (2 \operatorname{sgn}(\eta_{xyr}'') |\eta_{xy}''| / (\eta_{xx}'' - \eta_{yy}'')), \quad (22)$$

where $|\cdot|$ denotes magnitude and $\text{sgn}(\eta_{xyr}'')$ is the sign of η_{xyr}'' . The phase velocity indices are

$$\begin{aligned} n_1 &= (\eta_{xx}'' \cos^2 \Phi + \eta_{yy}'' \sin^2 \Phi + 2 \text{sgn}(\eta_{xyr}'') |\eta_{xy}''| \cos \Phi \sin \Phi)^{-\frac{1}{2}} \\ n_2 &= (\eta_{xx}'' \sin^2 \Phi + \eta_{yy}'' \cos^2 \Phi - 2 \text{sgn}(\eta_{xyr}'') |\eta_{xy}''| \cos \Phi \sin \Phi)^{-\frac{1}{2}}. \end{aligned} \quad (23)$$

The corresponding states of polarization are just the rows of the 2×2 unitary transformation matrix of Eq. (18):

$$\begin{aligned} D_1 &= [\cos \Phi \quad e^{iB} \sin \Phi]^H \\ D_2 &= [-e^{-iB} \sin \Phi \quad \cos \Phi]^H, \end{aligned} \quad (24)$$

where $B = \text{Arg}(\eta_{xy}'')$. These states are the left eigenvectors of $[\eta]''$; the right eigenvectors are the complex conjugate transpose of Eq. (24) and are

$$D_1 = \begin{bmatrix} \cos \Phi \\ e^{-iB} \sin \Phi \end{bmatrix}, \quad D_2 = \begin{bmatrix} -e^{iB} \sin \Phi \\ \cos \Phi \end{bmatrix}. \quad (25)$$

The orthogonality relation, $D_1 \cdot D_2^* = 0$, is satisfied. From Eq. (23) if $n_1 < n_2$, as shown in Fig. 7, then D_1 is the "fast" wave and D_2 is the "slow" wave. If $n_1 > n_2$, then the "fast" and "slow" waves are reversed.

Now the full description of these eigen-polarizations must be determined; i.e., azimuth angle, ellipticity, and handedness. They have the same ellipticity but opposite senses of rotation with orthogonal major axes. First, the azimuth angle or direction of the major axes for D_1 and D_2 is easily obtained from Eq. (22) as follows. The orthogonal transformation performed on $[\eta]'$ can be visualized in terms of the index ellipsoid. The cross-section ellipse transverse to k is found by taking only the real part of the transformed tensor $[\eta]''$, giving $X''^T \text{Re}([\eta]'') X'' = 1$, or

$$\eta_{xx}''x''^2 + \eta_{yy}''y''^2 + 2\eta_{xyr}''x''y'' = 1, \quad (26)$$

where $\text{Re}([\eta]'')$ is the real part of $[\eta]''$ and $\mathbf{X}'' = [x'' \ y'']^T$. The azimuth angle β_1 for D_1 is the angle in the real Cartesian (x'', y'') plane required to diagonalize $\text{Re}([\eta]'')$. It is

$$\beta_1 = \frac{1}{2} \text{Tan}^{-1} [2\eta_{xyr}'' / (\eta_{xx}'' - \eta_{yy}'')]. \quad (27)$$

This expression is the same as Eq. (22) if the numerator $2\text{sgn}(\eta_{xyr}'') |\eta_{xy}''|$ is replaced by $2\eta_{xyr}''$. The azimuth angle for D_2 is just $\beta_2 = \beta_1 + \pi/2$. The angles β_1 and β_2 define the orthogonal semi-axes directions (x''' and y''' in Fig. 7) of the cross-section ellipse of the index ellipsoid. If $\text{Im}(\eta_{xy}'')$ were zero, the lengths of the semi-axes would correspond to the phase velocity indices for the two linear polarizations. These indices would be calculated from Eq. (23) with β_1 rather than Φ .

The ellipticity and handedness of D_1 and D_2 can be found through the use of a complex polarization variable (CPV) χ .³¹ These eigen-polarizations are in the form of a two-component Cartesian Jones vector orthogonal to \mathbf{k} :

$$D_1 = \begin{bmatrix} D_x \\ D_y \end{bmatrix}_1 = \begin{bmatrix} |D_x| e^{i\delta_x} \\ |D_y| e^{i\delta_y} \end{bmatrix}_1. \quad (28)$$

The form of the CPV is then $\chi = r \exp(i\Delta\delta)$, where $r = |D_y/D_x|$ and $\Delta\delta = \delta_y - \delta_x$. It performs a bilinear transformation from the complex (x'', y'') plane to polarization space, shown in Fig. 8, where points in the complex χ plane represent polarization states. This plane, in fact, maps directly onto the Poincare' sphere. The equator of the sphere is the horizontal real axis of linear polarizations, and the north and south poles are the points R and L of the right- and left-circular polarizations, respectively. From D_1 , the CPV is

$$\chi_1 = e^{-iB} \tan \Phi, \quad (29)$$

and from the orthogonal state D_2 ,

$$\chi_2 = -1/\chi_1^* = -e^{-iB} \cot \Phi. \quad (30)$$

Relationships between the CPV χ_1 and the azimuth angle β_1 and ellipticity angle ξ_1 are given by Azzam and Bashara³¹ as

$$\begin{aligned} \tan 2\beta_1 &= 2\text{Re}(\chi_1)/(1 - |\chi_1|^2) \\ \sin 2\xi_1 &= 2\text{Im}(\chi_1)/(1 + |\chi_1|^2). \end{aligned} \quad (31)$$

In terms of the impermeability tensor elements and the rotation angle Φ , the azimuth angle β_1 was given in Eq. (27), and the ellipticity angle ξ_1 was derived to be $\sin 2\xi_1 = -(\text{Im}(\eta_{xy}''')/|\eta_{xy}|) \sin 2\Phi = -\sin B \sin 2\Phi$ or

$$\xi_1 = -\frac{1}{2} \sin^{-1}(\sin B \sin 2\Phi). \quad (32)$$

The ellipticity is given by $\tan \xi_1$. Furthermore, the relative amplitude of the orthogonal components of D_1 is defined as $r_1 = \tan \Phi$, and the relative phase is $\Delta\delta_1 = -\text{Arg}(\eta_{xy}''') = -B$.

The handedness of the polarization is determined by the sign of the relative phase. If $\Delta\delta$ is > 0 , then the elliptical polarization is left-handed. If $\Delta\delta < 0$, then the polarization is right-handed. And if $\Delta\delta = 0$ or $m\pi$, $m = 1, 2, 3, \dots$, then the polarization is linear.

For the orthogonal polarization state, the parameters β_2 , ϵ_2 , r_2 , and $\Delta\delta_2$ for χ_2 are³¹

$$\beta_2 = \beta_1 + \pi/2, \quad \xi_2 = -\xi_1, \quad r_2 = \cot \Phi, \quad \Delta\delta_2 = -\pi + \Delta\delta_1. \quad (33)$$

The orthogonality condition for χ_1 and χ_2 is $\chi_1 \chi_2^* = -1$. Therefore, in the

process of diagonalizing a Hermitian matrix, the relative phase $\Delta\delta$ and ellipticity angle ξ are changing iteratively. In the case of a real symmetric matrix, the process is interpreted as a rigid body rotation.¹

The advantages of this method include the following: (1) It is accurate and stable for all crystal classes; (2) Stable orthonormal eigenvectors are found simultaneously with the eigenvalues; (3) The unitary transformation matrix is easily determined by elements of the perturbed impermeability tensor; (4) All descriptive information about the eigen-polarizations of a crystal for a given k is obtained from the unitary transformation matrix with simple formulas; and (5) The combined effects of real and Hermitian perturbations to the impermeability tensor can be straightforwardly handled.

V. Example: The Sillenite Crystal Class

A cubic sillenite crystal of class 23 is examined to illustrate the ease and accuracy of the method just described. This crystal class is being widely investigated for applications in dynamic real-time holographic interferometry and spatial light modulation.^{23,32} The class includes bismuth silicon oxide (BSO), bismuth germanium oxide (BGO), and bismuth titanium oxide (BTO). These crystals are electro-optic, optically active, electrogyratory, piezoelectric, and elasto-optic. The electro-optic effect, optical activity, and electrogyration effect combined may strongly affect the polarization in these crystals. BSO is examined to illustrate these influences on the eigen-polarizations.

Two principal configurations of BSO, both transverse, are used for volume holography. One of them is shown in Fig. 9.³² An external electric bias is applied in the $[\bar{1}\bar{1}0]$ direction, and the direction of light propagation is $[\bar{1}10]$ or $(\phi_k, \theta_k) = (135^\circ, 90^\circ)$. In the (x,y,z) coordinate system, the unperturbed impermeability tensor for this cubic isotropic

crystal is

$$[1/n^2] = \begin{bmatrix} 1/n_0^2 & 0 & 0 \\ 0 & 1/n_0^2 & 0 \\ 0 & 0 & 1/n_0^2 \end{bmatrix}, \quad (34)$$

where n_0 is the principal refractive index of the crystal. The index ellipsoid is a sphere. The gyration tensor for natural optical activity is a function of the given applied electric field and wavevector directions and is

$$[g]' = \begin{bmatrix} g_{11} & 0 & \zeta_{41} E_y \\ 0 & g_{11} & \zeta_{41} E_x \\ \zeta_{41} E_y & \zeta_{41} E_x & g_{11} \end{bmatrix}, \quad (35)$$

where ζ_{41} is the electrogyratory coefficient. The gyration surface changes from a sphere to the surface (from Eqs. (8) and (17)),

$$G' = g_{11} - \sqrt{2} \zeta_{41} E \sin\theta_k \cos\theta_k (\sin\phi_k + \cos\phi_k), \quad (36)$$

where $E_x = E_y = -1/\sqrt{2} E$, and E is the magnitude of applied field. If $E = 0$, then $G' = G = g_{11}$, which is a sphere. The perturbed gyration surface is shown in Fig. 10. Note by Eq. (36) that for the given field ($[\bar{1} \bar{1} 0]$) and wavevector ($[\bar{1} 1 0]$) directions, the effect of electrogyration is not present. Therefore, with the electro-optic effect, optical activity, and the given direction of propagation k taken into account, the tensor becomes

$$[\eta]' = \begin{bmatrix} 1/n_0^2 & 0 & 1/\sqrt{2}(-r_{41}E - ig_{11}/n_0^4) \\ 0 & 1/n_0^2 & 1/\sqrt{2}(-r_{41}E - ig_{11}/n_0^4) \\ 1/\sqrt{2}(-r_{41}E + ig_{11}/n_0^4) & 1/\sqrt{2}(-r_{41}E + ig_{11}/n_0^4) & 1/n_0^2 \end{bmatrix}, \quad (37)$$

where $G_x = -G_y = -1/\sqrt{2} g_{11}$. The new orientation of the index ellipsoid is obtained by applying the general Jacobi method as described in Ref. 1 to the

real part of Eq. (37). The crystal is now biaxial, and the principal indices and axes are

$$\begin{aligned} n_{x'} &= 2.52996 & x' &= [1/2 \quad 1/2 \quad -1/\sqrt{2}]^T \\ n_{y'} &= 2.53 & y' &= [-1/\sqrt{2} \quad 1/\sqrt{2} \quad 0]^T \quad (y' \parallel \mathbf{k}) \\ n_{z'} &= 2.53004 & z' &= [1/2 \quad 1/2 \quad 1/\sqrt{2}]^T. \end{aligned} \quad (38)$$

To determine the eigenstates of the crystal for the given \mathbf{k} , the entire $[\eta]'$ tensor of Eq. (37) must be transformed to the (x'', y'', z'') coordinate system by Eqs. (19). The resulting 2 x 2 matrix in the (x'', y'') plane is given by

$$[\eta]'' = \begin{bmatrix} 1/n_0^2 & (-r_{41}E + ig_{11}/n_0^4) \\ (-r_{41}E - ig_{11}/n_0^4) & 1/n_0^2 \end{bmatrix}, \quad (39)$$

and $x'' = -z$ ($[0 \quad 0 \quad \bar{1}]$), $y'' = -1/\sqrt{2} x - 1/\sqrt{2} y$ ($[\bar{1} \quad \bar{1} \quad 0]$), and $z'' = -1/\sqrt{2} x + 1/\sqrt{2} y$ ($[\bar{1} \quad 1 \quad 0] \parallel \mathbf{k}$). The cross-section ellipse is, by Eq. (26),

$$1/n_0^2 (x''^2 + y''^2) - 2r_{41}E x''y'' = 1. \quad (40)$$

The azimuth angle is found by placing this cross-section in principal coordinates, i.e., by diagonalizing the real part of Eq. (39). This angle is $\beta_1 = \frac{1}{2}\text{Tan}^{-1}(-2r_{41}E/(1/n_0^2 - 1/n_0^2)) = -45^\circ$. Therefore, the axes of the cross-section ellipse are along $x''' = [1/2 \quad 1/2 \quad -1/\sqrt{2}]^T$ and $y''' = [-1/2 \quad -1/2 \quad -1/\sqrt{2}]^T$. Numerical values³² for the various parameters are $n_0 = 2.53$ and $r_{41} = 4.41 \times 10^{-12}$ m/V at a freespace wavelength of $\lambda_0 = 0.6328 \mu\text{m}$. From these numbers the lengths of the principal axes are $n_{x'''} = n_0 - \frac{1}{2}n_0^3 r_{41}E = 2.52996$ and $n_{y'''} = n_0 + \frac{1}{2}n_0^3 r_{41}E = 2.53004$ for a field magnitude of 10^6 V/m.

The phase velocity indices are found by diagonalizing the entire matrix $[\eta]''$ of Eq. (39). The required rotation angle is

$$\Phi = \frac{1}{2} \tan^{-1} (2 \operatorname{sgn}(\eta_{xy}) |\eta_{xy}''| / (1/n_0^2 - 1/n_0'^2)) = -45^\circ, \quad (41)$$

and $|\eta_{xy}''| = ((r_{41}E)^2 + (g_{11}/n_0^4)^2)^{1/2}$. The constant g_{11} is calculated from the measured specific rotation of $\rho = 21.4^\circ/\text{mm}$ (Ref. 32) which is equal to $\pi g_{11}/\lambda n_0$. Therefore, $g_{11}/n_0^4 = \lambda \rho / \pi n_0^3 = 2.6618 \times 10^{-4}$, giving $|\eta_{xy}''| = 2.6621 \times 10^{-4}$. Optical activity dominates the magnitude of the off-diagonal element η_{xy}'' . The phase velocity indices are found from Eqs. (23) to be,

$$\begin{aligned} n_1 &= (1/n_0^2 + |\eta_{xy}''|)^{-1/2} = 2.52785 \quad (\text{fast wave}) \\ n_2 &= (1/n_0^2 - |\eta_{xy}''|)^{-1/2} = 2.53216. \quad (\text{slow wave}) \end{aligned} \quad (42)$$

The circular (elliptical) birefringence is then $\Delta n_c = n_2 - n_1 = 0.0043111$. Without the electric field applied, the indices are $n_1 = 2.52785$ ($= n_1$) and $n_2 = 2.532158$ ($< n_2$), giving a circular birefringence of $\Delta n_c = n_2 - n_1 = 0.0043080$. Therefore, the electro-optic effect only slightly enhances circular birefringence. The corresponding eigenvectors are found from Eq. (25) to be

$$D_1 = \begin{bmatrix} 1/\sqrt{2} \\ -(0.01656 + i0.99986)1/\sqrt{2} \end{bmatrix}, \quad D_2 = \begin{bmatrix} (0.01656 - i0.99986)1/\sqrt{2} \\ 1/\sqrt{2} \end{bmatrix}, \quad (43)$$

and $B = \operatorname{Arg}(\eta_{xy}'') = -89.0508^\circ$.

The CPV χ_1 is $-\exp(-iB)$. From Eq. (31), the azimuth angle is $\beta_1 = -45^\circ$, which agrees with the angle obtained before. Also from Eq. (31), the ellipticity angle is $\sin 2\xi_1 = \operatorname{Im}(\chi_1) = \sin B$, which is equal to $-\operatorname{Im}(\eta_{xy}'')/|\eta_{xy}''| \sin 2\Phi = -\sin B \sin 2\Phi = \sin B$ from Eq. (32) for $\Phi = -45^\circ$. Therefore, Eqs. (31) and (32) are consistent. The ellipticity angle is then -44.52541° and the ellipticity of the polarization is $\tan \xi_1 = -0.98357^\circ$ (almost circular polarization). The relative amplitude is $r_1 = 1$, and the relative phase between D_{x1} and D_{y1} is $\Delta \delta_1 = +89.05^\circ$. The corresponding point

on the complex χ plane in Fig. 8 is on the unit circle at the phase angle of $+89.05^\circ$. Since $\Delta\delta_1 > 0$, then D_1 is left-handed polarization, and $n_1 = n_l$ is the corresponding index. Therefore, D_1 corresponds to the fast wave.

For the orthogonal polarization D_2 , the CPV is $\chi_2 = \exp(-iB)$. The azimuth angle is $+45^\circ$, and the ellipticity angle is $-\xi_1$ or $+44.52541^\circ$ for an ellipticity of 0.98357. The relative amplitude is $r_2 = 1$, and the relative phase between D_{x_2} and D_{y_2} is -90.95° . The corresponding point on the complex χ plane in Fig. 8 is on the unit circle at the phase angle of -90.95° . Since the $\Delta\delta_2 < 0$, D_2 is right-handed polarization, and $n_2 = n_R$. Therefore, D_2 corresponds to the slow wave.

Finally, an additional note is that the phase retardation, Γ , between D_1 and D_2 for a given crystal thickness d may be calculated from the circular (elliptical) birefringence Δn_c . It is given by $\Gamma = 2\pi/\lambda \Delta n_c d$ and in general, includes the effects of both the natural optical activity and the external electric field (e.g., electro-optic and electrogyration effects).

VI. Conclusion

A straightforward systematic procedure for performing electro-optic effect calculations was developed and presented in Ref. 1. That approach, which employs the general Jacobi method, can be used to analyze propagation in electro-optic materials in any crystal class for an arbitrary electric field direction and arbitrary wavevector direction. The properties of the impermeability tensor were exploited to arrive at simple, stable, and accurate expressions for determining the principal axes and indices of a crystal and the eigenstates (phase velocity indices and eigen-polarizations) for a given direction of propagation k .

In this paper that procedure has been extended to gyrotropic crystals. External (or internal) influences, such as optical activity, electrogyration

effect, and Faraday rotation may now be included, singly or together. These circular birefringence effects are more complicated and, in general, produce elliptical eigen-polarizations. The extended method requires a unitary transformation from a Cartesian coordinate system to a complex helical coordinate system to determine the eigenstates for a given direction of propagation. Using a unitary matrix suggested by Wilkinson,²⁸ a set of formulas has been derived which results in an extended version of the general Jacobi method applicable to Hermitian matrices. These relationships are given in the Appendix. Furthermore, a complex polarization variable was introduced to quantify the connection between the elements of the perturbed impermeability tensor and the eigen-polarizations. This new procedure reduces easily to the less complicated case where the electro-optic effect alone is present.

More specifically, two questions were posed and answered in the present work:

- 1) Given a crystal that is linear birefringent (natural or induced) and/or gyrotropic (natural or induced), what are the principal refractive indices and principal dielectric axes of the crystal?
- 2) What are the eigenstates for an arbitrary direction of light propagation?

The step-by-step procedure introduced in this paper is summarized as follows:

- 1) The general Jacobi method as described in Ref. 1 is applied to the real part of the perturbed impermeability tensor $[\eta]'$ to determine the principal indices and axes of the crystal.
- 2) A real orthogonal transformation is performed on $[\eta]'$ to place the tensor in the coordinate system of $k(x'',y'',z'')$, giving $[\eta]''$.
- 3) Using formulas from the Appendix, the eigenstates for the given k

are obtained.

- 4) From the eigenvectors of $[\eta]''$ a complex polarization variable (CPV) is defined. Using the CPV, the descriptive properties of the eigen-polarizations, i.e., azimuth angle, ellipticity and handedness, are determined in terms of the elements of $[\eta]''$.

To provide a geometric interpretation of linear and circular birefringence, the index ellipsoid and gyration surface were used.

Finally, the sillenite crystal class was examined to illustrate the ease and accuracy of the extended method. Specifically, bismuth silicon oxide (BSO) was analyzed in a principal configuration to show the effects of its natural optical activity together with the simultaneous influences of an applied electric field (through the electrogyration and electro-optic effects) on the eigenstates of the crystal for a given k . Example numerical results were presented.

Appendix: Complex Plane Rotations

The general Jacobi method is modified here for diagonalizing a 3×3 Hermitian matrix. This iterative procedure involves a unitary transformation from a Cartesian to a helical coordinate system. As a quick reference the following relationships for the rotation angle, the unitary transformation matrix, and the updated impermeability elements are provided for rotation in each of the three complex planes. These expressions are derived from the coordinate transformation law for second-rank tensors. The rotation angle in the complex (x,y) principal plane is denoted by ϕ , in the complex (x,z) principal plane by θ , and in the complex (y,z) principal plane by ψ . The impermeability tensor is represented as the Hermitian matrix H.

1. Rotation in the complex (x,y) plane.

The rotation angle ϕ required to zero the H_{12} element is found by

$$\phi = \frac{1}{2} \tan^{-1} [2|H_{12}| / (H_{11} - H_{22})]. \quad (A1)$$

This angle represents a counterclockwise rotation in the complex (x,y) plane. The transformation matrix is

$$[a]_{\phi} = \begin{bmatrix} \cos\phi & e^{iA} \sin\phi & 0 \\ -e^{-iA} \sin\phi & \cos\phi & 0 \\ 0 & 0 & 1 \end{bmatrix}, \quad (A2)$$

where $\exp(iA) = H_{12} / |H_{12}|$. The elements of H are updated as follows:

$$\begin{aligned} H_{\phi 11}' &= H_{11} \cos^2 \phi + H_{22} \sin^2 \phi + 2|H_{12}| \cos\phi \sin\phi \\ H_{\phi 22}' &= H_{11} \sin^2 \phi + H_{22} \cos^2 \phi - 2|H_{12}| \cos\phi \sin\phi \\ H_{\phi 33}' &= H_{33} \\ H_{\phi 12}' &= (H_{22} - H_{11})(H_{12}/|H_{12}|) \cos\phi \sin\phi + H_{12}(\cos^2 \phi - \sin^2 \phi) - H_{21}'^* = 0 \\ H_{\phi 13}' &= H_{13} \cos\phi + H_{23}(H_{12}/|H_{12}|) \sin\phi - H_{31}'^* \\ H_{\phi 23}' &= -H_{13}(H_{12}^*/|H_{12}|) \sin\phi + H_{23} \cos\phi - H_{32}'^*. \end{aligned} \quad (A3)$$

2. Rotation in the complex (x,z) plane.

The rotation angle θ required to zero the H_{13} element is found by

$$\theta = \frac{1}{2} \tan^{-1} [2|H_{13}| / (H_{11} - H_{33})] \quad (A4)$$

This angle represents a clockwise rotation in the complex (x,z) plane. The transformation matrix is

$$[a]_{\theta} = \begin{bmatrix} \cos\theta & 0 & e^{iB} \sin\theta \\ 0 & 1 & 0 \\ -e^{-iB} \sin\theta & 0 & \cos\theta \end{bmatrix}. \quad (A5)$$

where $\exp(iB) = H_{13} / |H_{13}|$. The elements of H are updated as follows:

$$\begin{aligned} H_{\theta 11}' &= H_{11} \cos^2 \theta + H_{33} \sin^2 \theta + 2|H_{13}| \cos\theta \sin\theta \\ H_{\theta 22}' &= H_{22} \\ H_{\theta 33}' &= H_{11} \sin^2 \theta + H_{33} \cos^2 \theta - 2|H_{13}| \cos\theta \sin\theta \\ H_{\theta 12}' &= H_{12} \cos\theta + H_{23}^* (H_{13} / |H_{13}|) \sin\theta - H_{21}^* \\ H_{\theta 13}' &= (H_{33} - H_{11}) (H_{13} / |H_{13}|) \cos\theta \sin\theta + H_{13} (\cos^2 \theta - \sin^2 \theta) - H_{31}^* \sin\theta \\ H_{\theta 23}' &= -H_{12}^* (H_{13} / |H_{13}|) \sin\theta + H_{23} \cos\theta - H_{32}^* \sin\theta. \end{aligned} \quad (A6)$$

3. Rotation in the complex (y,z) plane.

The rotation angle ψ required to zero the H_{23} element is found by

$$\psi = \frac{1}{2} \tan^{-1} [2|H_{23}| / (H_{22} - H_{33})]. \quad (A7)$$

This angle represents a counterclockwise rotation in the complex (y,z) plane. The transformation matrix is

$$[a]_{\psi} = \begin{bmatrix} 1 & 0 & 0 \\ 0 & \cos\psi & e^{iC} \sin\psi \\ 0 & -e^{-iC} \sin\psi & \cos\psi \end{bmatrix}. \quad (A8)$$

where $\exp(iC) = H_{23} / |H_{23}|$. The elements of H are updated as follows:

$$H_{\psi 11}' = H_{11}$$

$$H_{\psi 22}' = H_{22} \cos^2 \psi + H_{33} \sin^2 \psi + 2 |H_{23}| \cos \psi \sin \psi$$

$$H_{\psi 33}' = H_{22} \sin^2 \psi + H_{33} \cos^2 \psi - 2 |H_{23}| \cos \psi \sin \psi$$

(A9)

$$H_{\psi 12}' = H_{12} \cos \psi + H_{13} (H_{23}^* / |H_{23}|) \sin \psi - H_{21}'^*$$

$$H_{\psi 13}' = -H_{12} (H_{23} / |H_{23}|) \sin \psi + H_{13} \cos \psi - H_{31}'^*$$

$$H_{\psi 23}' = (H_{33} - H_{22}) (H_{23} / |H_{23}|) \cos \psi \sin \psi + H_{23} (\cos^2 \psi - \sin^2 \psi) - H_{32}'^* = 0.$$

References

1. T. A. Maldonado and T. K. Gaylord, "Electro-optic Effect Calculations: A Simplified Procedure for Arbitrary Cases," submitted to *Appl. Opt.*, manuscript no. 1407, received July 7, 1988.
2. A. Yariv, "Coupled-Mode Theory for Guided-Wave Optics," *IEEE J. Quantum Electron.* QE-9, 919 (1973).
3. A. Yariv and J. F. Lotspeich, "Coupled-Mode Analysis of Light Propagation in Optically Active Crystals," *J. Opt. Soc. Am.* 72, 273 (1982).
4. P. Van Den Keybus and W. Grevendonk, "Comparison of Optical Activity and Faraday Rotation in Crystalline SiO_2 ," *Phys. Stat. Sol. B* 136, 651 (1986).
5. M. P. Silverman, "Effects of Circular Birefringence on Light Propagation and Reflection," *Am. J. Phys.* 54, 69 (1986).
6. S. Mallick, D. Rouede, and A. G. Apostolidis, "Efficiency and Polarization Characteristics of Photorefractive Diffraction in a $\text{Bi}_{12}\text{SiO}_{20}$ Crystal," *J. Opt. Soc. Am. B* 4, 1247 (1987).
7. A. Marrakchi, R. V. Johnson, and A. R. Tanguay, "Polarization Properties of Photorefractive Diffraction in Electrooptic and Optically Active Sillenite Crystals (Bragg Regime)," *J. Opt. Soc. Am.* 3, 321 (1986).
8. O. S. Eritsyian, "Optical problems in the electrodynamics of gyrotropic Media," *Sov. Phys. Usp.* 25, 919 (1983).
9. E. U. Condon, "Theories of Optical Rotatory Power," *Rev. Mod. Phys.* 9, 432, (1937).
10. D. Eimerl, "Quantum Electrodynamics of Optical Activity in Birefringent Crystals," *J. Opt. Soc. Am. B* 5, 1453 (1988).
11. R. M. Hornreich and S. Shtrikman, "Theory of Gyrotropic Birefringence," *Phys. Rev.* 171, 1065 (1968).
12. M. Born and E. Wolf, *Principles of Optics* (Pergamon Press, New York, 1959).

13. A. Yariv and P. Yeh, *Optical Waves in Crystals* (Wiley, New York, 1983).
14. L. D. Landau and E. M. Lifshitz, *Electrodynamics of Continuous Media* (Pergamon, London, 1960).
15. J. F. Nye, *Physical Properties of Crystals* (Oxford University Press, London, 1957).
16. V. M. Agranovich and V. L. Ginzburg, *Crystal Optics with Spatial Dispersion, and Excitons* (Springer-Verlag, New York, 1984).
17. A. V. Shubnikov, *Principles of Optical Crystallography* (Consultants Bureau, New York, 1960).
18. V. M. Agranovich and V. L. Ginzburg, "Phenomenological Electrodynamics of Gyrotropic Media," *Sov. Phys. JETP* 36, 440 (1973).
19. B. V. Bokut' and A. N. Serdyukov, "On the Phenomenological Theory of Natural Optical Activity," *Sov. Phys. JETP* 34, 962 (1972).
20. A. Yariv, *Optical Electronics* (Holt, Rinehart, and Winston, New York, 1976).
21. O. G. Vlokh, "Electrogyration properties of crystals," *Ferroelectrics* 75, 119 (1987).
22. J. Kobayashi, T. Asahi, and S. Takahashi, "Simultaneous Measurements of Electrogyration and Electrooptic Effects of α -quartz," *Ferroelectrics* 75, 139 (1987).
23. F. Vachss and L. Hesselink, "Measurement of the Electrogyratory and Electro-optic Effects in BSO and BGO," *Opt. Comm.* 62, 159 (1987).
24. F. A. Hopf and G. I. Stegeman, *Applied Classical Electrodynamics, Vol. 1: Linear Optics* (Wiley, New York, 1985).
25. M. J. Freiser, "A Survey of Magneto-optic Effects," *IEEE Trans. Mag.* MAG-4, 152 (1968).
26. P. S. Pershan, "Magneto-optical Effects," *J. Appl. Phys.* 38, 1482 (1967).

27. J. F. Dillon, "Magneto-optics and its Uses," *J. Mag. and Mag. Mat.* 31-34, 1 (1983).
28. J. H. Wilkinson, *The Algebraic Eigenvalue Problem* (Oxford University Press, London, 1965).
29. P. Hlawiczka, *Gyrotropic Waveguides* (Academic Press, New York, 1981).
30. *IMSL Library Reference Manual* (International Mathematical and Statistical Libraries, Inc., Houston, TX, ed. 9.2, 1980).
31. R. M. A. Azzam and N. M. Bashara, *Ellipsometry and Polarized Light* (Elsevier Science, New York, 1987).
32. A. Marrakchi, R. V. Johnson, and A. R. Tanguay, "Polarization Properties of Photorefractive Diffraction in Electro-optic and Optically Active Sillenite Crystals (Bragg Regime)," *J. Opt. Soc. Am. B* 3, 321 (1986).

Table I. Gyration tensors g_{ij} for all crystal classes exhibiting natural optical activity. (Ref. 13)

| Triclinic | | Monoclinic | | Orthorhombic | |
|--|--|---|--|---|--|
| 1 | 2 (2 y) | m (m ⊥ y) | 222 | 2mm | |
| $\begin{bmatrix} g_{11} & g_{12} & g_{13} \\ g_{21} & g_{22} & g_{23} \\ g_{31} & g_{32} & g_{33} \end{bmatrix}$ | $\begin{bmatrix} g_{11} & 0 & g_{13} \\ 0 & g_{22} & 0 \\ g_{13} & 0 & g_{33} \end{bmatrix}$ | $\begin{bmatrix} 0 & g_{12} & 0 \\ g_{12} & 0 & g_{23} \\ 0 & g_{23} & 0 \end{bmatrix}$ | $\begin{bmatrix} g_{11} & 0 & 0 \\ 0 & g_{22} & 0 \\ 0 & 0 & g_{33} \end{bmatrix}$ | $\begin{bmatrix} 0 & g_{12} & 0 \\ g_{12} & 0 & 0 \\ 0 & 0 & 0 \end{bmatrix}$ | |
| Uniaxial | | | | | |
| Tetragonal | | | Trigonal and Hexagonal | | |
| 4, 422 | $\bar{4}$ | $\bar{4}2m$ (2 x) | 3, 32, 622 | | |
| $\begin{bmatrix} g_{11} & 0 & 0 \\ 0 & g_{11} & 0 \\ 0 & 0 & g_{33} \end{bmatrix}$ | $\begin{bmatrix} g_{11} & g_{12} & 0 \\ g_{12} & -g_{11} & 0 \\ 0 & 0 & 0 \end{bmatrix}$ | $\begin{bmatrix} 0 & g_{12} & 0 \\ g_{12} & 0 & 0 \\ 0 & 0 & 0 \end{bmatrix}$ | $\begin{bmatrix} g_{11} & 0 & 0 \\ 0 & g_{11} & 0 \\ 0 & 0 & g_{33} \end{bmatrix}$ | | |
| Isotropic (without center of symmetry) | | | | | |
| Cubic | | | | | |
| 432, 23 | | | | | |
| $\begin{bmatrix} g_{11} & 0 & 0 \\ 0 & g_{11} & 0 \\ 0 & 0 & g_{11} \end{bmatrix}$ | | | | | |

FIGURE CAPTIONS

Fig. 1. The sense of optical rotation relative to the direction of propagation \mathbf{k} for (a) natural optical activity and (b) Faraday rotation.

Fig. 2. The index ellipsoid cross-section (cross-hatched) that is normal to the wavevector \mathbf{k} and passes through the origin. The principal axes of the cross-hatched ellipse represent the directions of the allowed linear polarizations D_1 and D_2 . D_1 , D_2 , and \mathbf{k} form an orthogonal triad.

Fig. 3. Gyration surface for right-handed quartz (class 32). The white surface depicts right-handed optical rotation with the maximum rotation occurring for propagation along the optic axis. The dark surface depicts left-handed rotation with maximum rotation along a direction perpendicular to the optic axis. There is no optical rotation for propagation $\sim 56^\circ$ from the optic axis.

Fig. 4. Gyration surface for Faraday active crystals. Maximum optical rotation occurs for propagation parallel and antiparallel to \mathbf{B} . The white surface depicts rotation of one sense while the dark surface depicts rotation of the opposite sense.

Fig. 5. The flattened helical contour of an elliptically polarized propagating wave at an instant of time. The radial vectors to the contour represent the displacement vector \mathbf{D} ($\perp \mathbf{k}$).

Fig. 6. Orthogonal transformation of the (x, y, z) dielectric axes to the (x'', y'', z'') coordinate system of the wavevector \mathbf{k} ($z'' \parallel \mathbf{k}$) represented in polar coordinates $(\phi_{\mathbf{k}}, \theta_{\mathbf{k}})$.

Fig. 7. The cross-section ellipse of the index ellipsoid in the (x'', y'') plane. The x''' and y''' axes represent the major axes of the eigenpolarizations oriented relative to x'' and y'' . The two eigenstates have orthogonal major axes, opposite handedness, and the same ellipticity. The

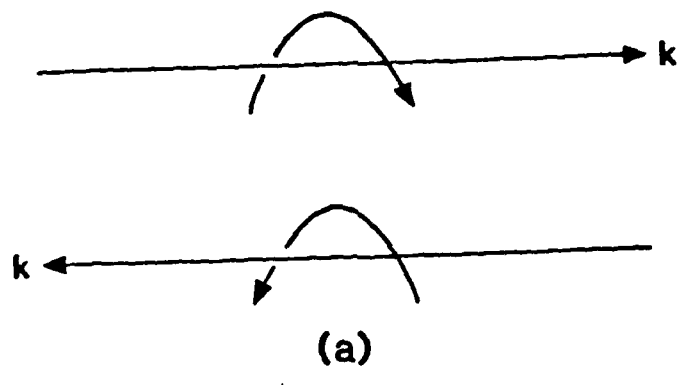
wavevector k and the z'' axis are normal to the plane of the figure.

Fig. 8. Cartesian complex plane of polarization. Each point in the plane represents a polarization state. The basis states are the horizontal linear polarization at the origin and the vertical linear polarization at infinity. The dashed circle represents the unit circle (unit relative amplitude). The radial line represents a contour of constant relative phase of $\pi/4$.

Fig. 9. A principal transverse crystal orientation of $\text{Bi}_{12}\text{SiO}_{20}$ (BSO). The external electric field is applied in the $[\bar{1}\bar{1}0]$ direction, and the direction of propagation is along $[\bar{1}10]$. The (x,y,z) coordinate system represents the unperturbed dielectric axes. The new coordinate system resulting from the electro-optic effect is represented by (x',y',z') . The coordinate system of the wavevector k is given by (x'',y'',z'') with $z'' \parallel k$. Finally, the (x''',y''',z''') coordinate system with $z''' \parallel z'' \parallel k$ represents the principal axis coordinate system of the eigenstates for the given k .

Fig. 10. Gyration surface for BSO in the (x,z) or (y,z) principal plane. The dashed circle represents the surface projection with no applied electric field, and therefore, the optical rotation is invariant with the wavevector k direction. The solid "heart-shape" contour depicts the the surface when a field is applied in the $[\bar{1}\bar{1}0]$ direction. The magnitude of radial vectors from the origin to the surface is a measure of the optical rotation per unit length which depends on the direction of k . Note that optical rotation is not affected by the electric field for propagation in the (x,y) plane.

OPTICAL ACTIVITY



FARADAY ROTATION

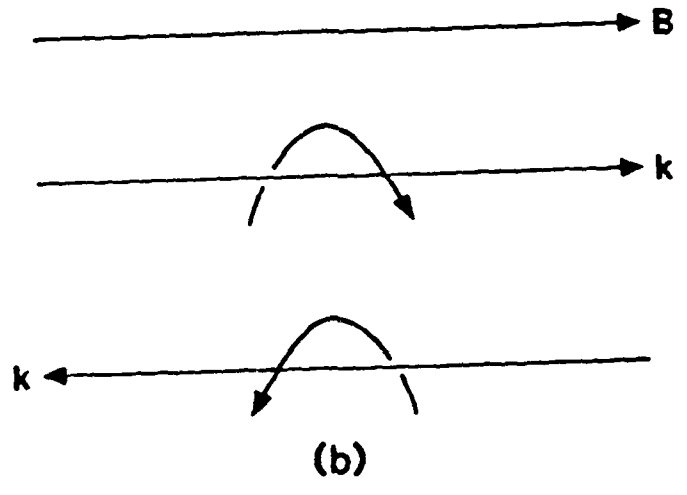


Fig.1

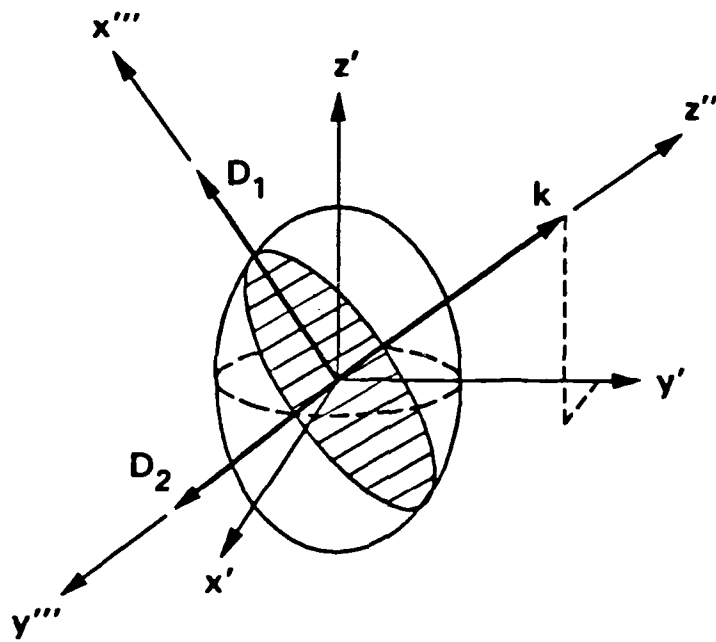


Fig. 2

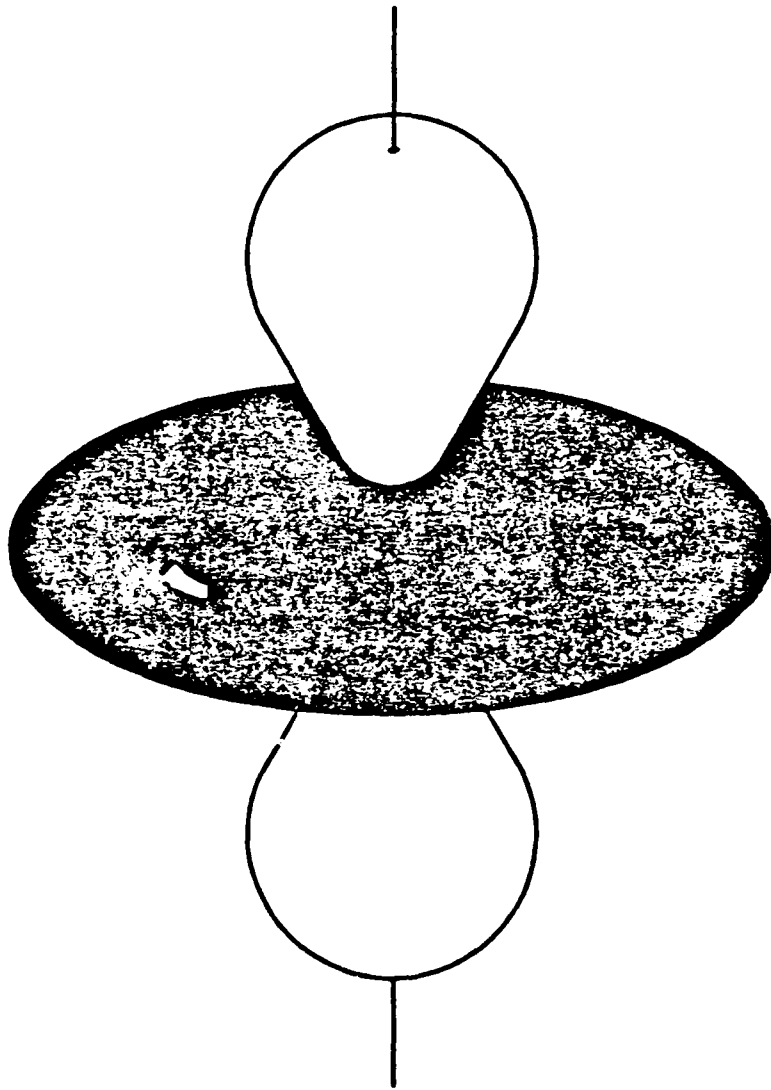


Fig. 3

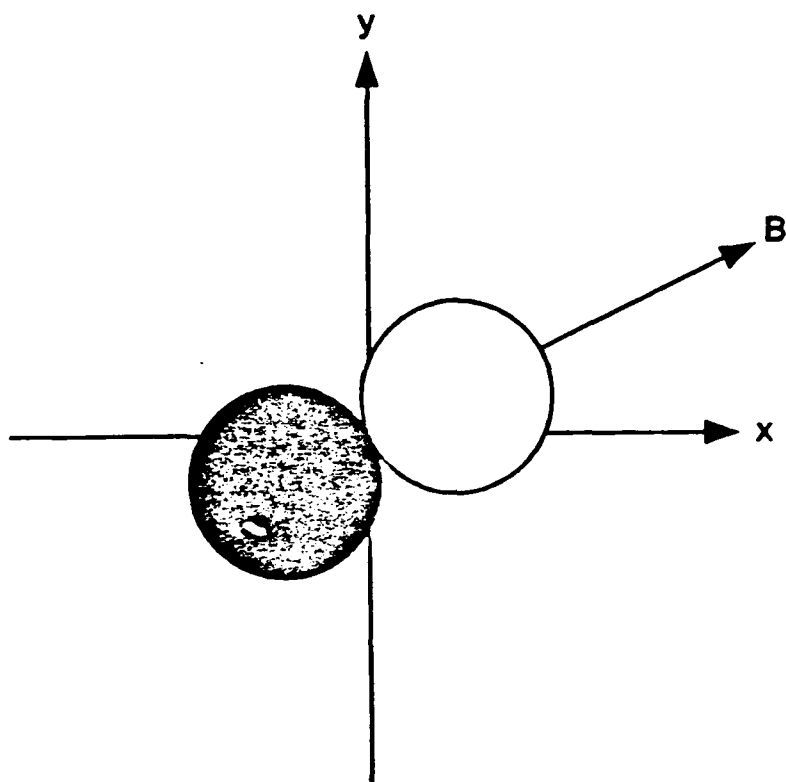


Fig. 4

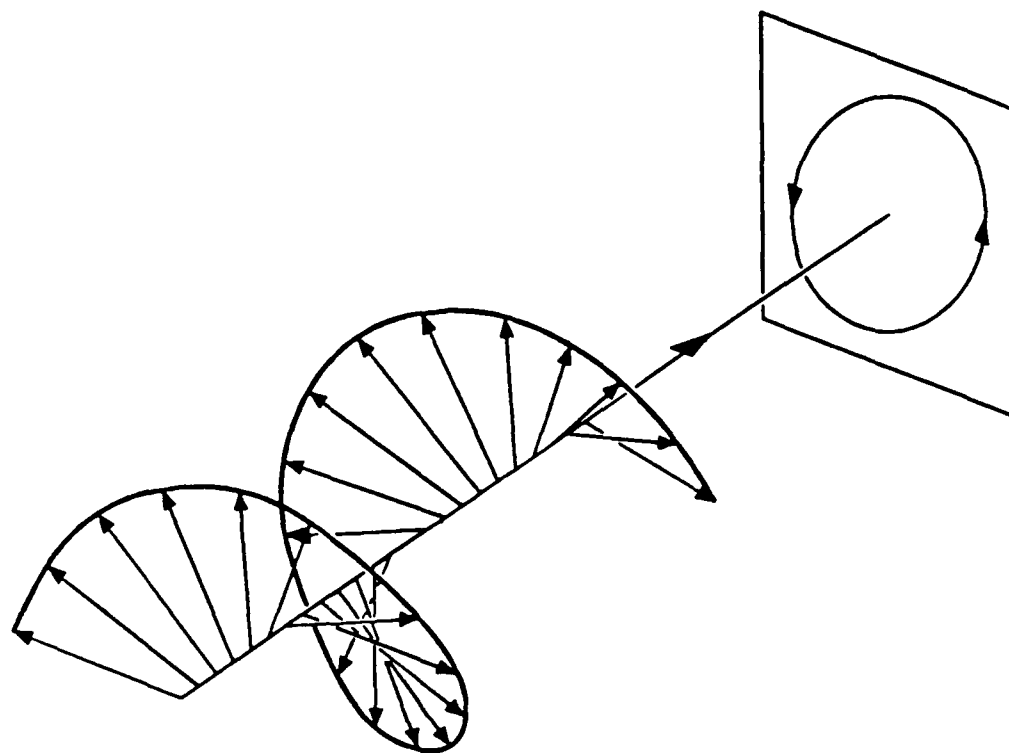


Fig. 5

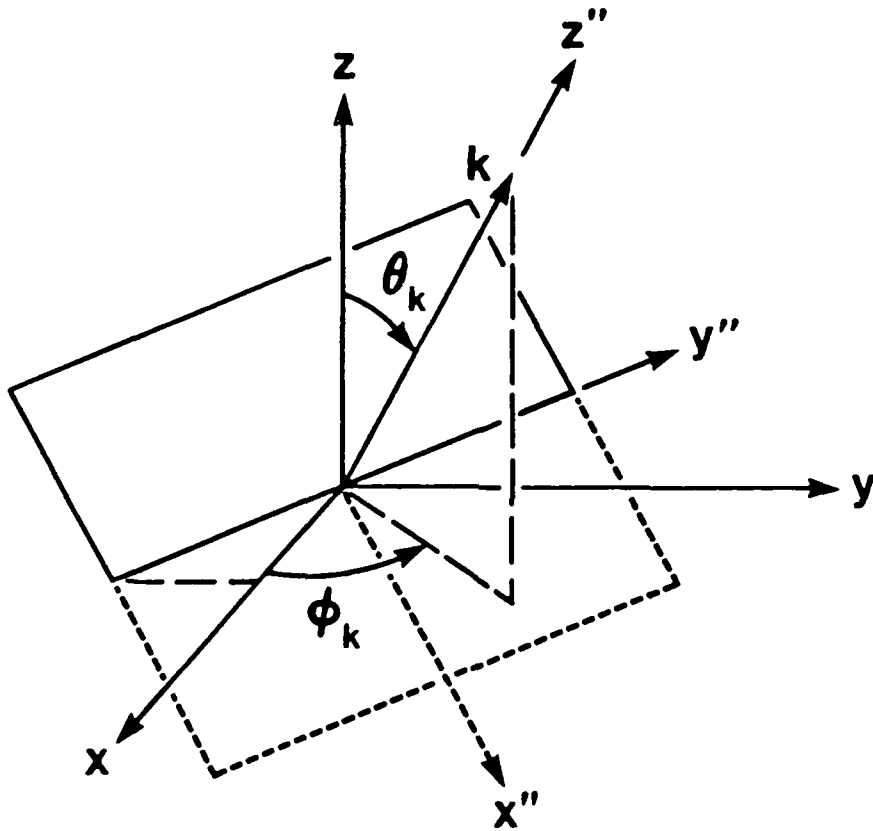


Fig. 6

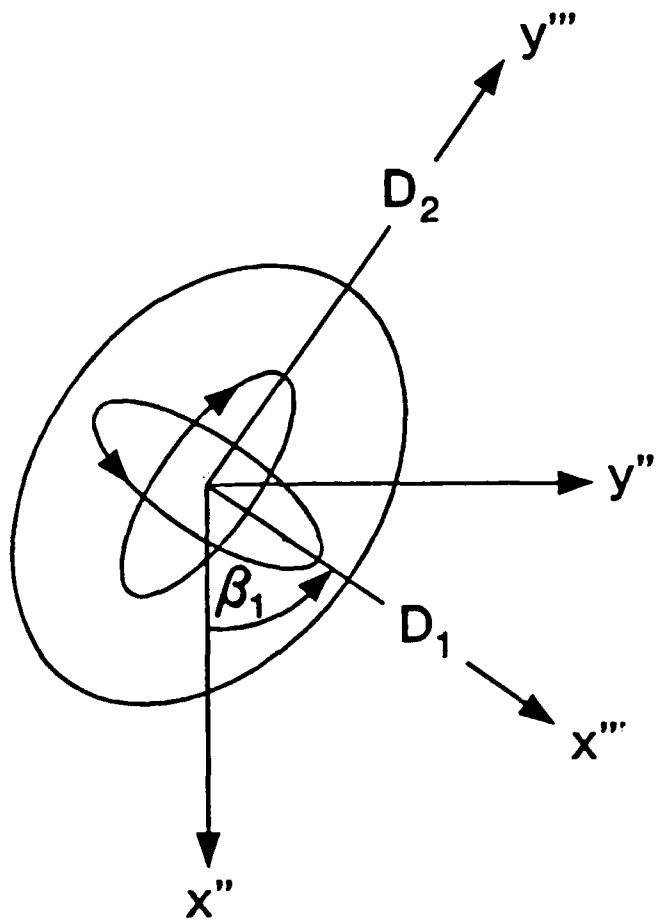


Fig. 7

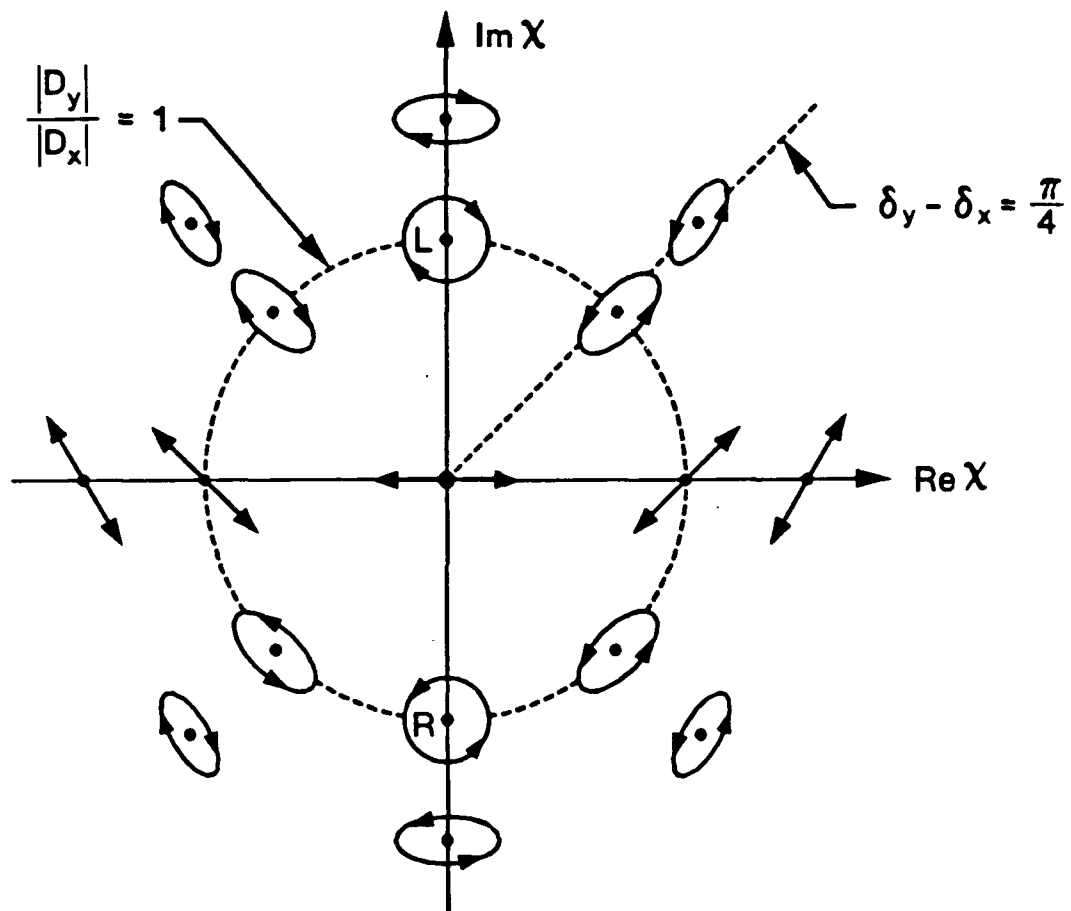


Fig. 8

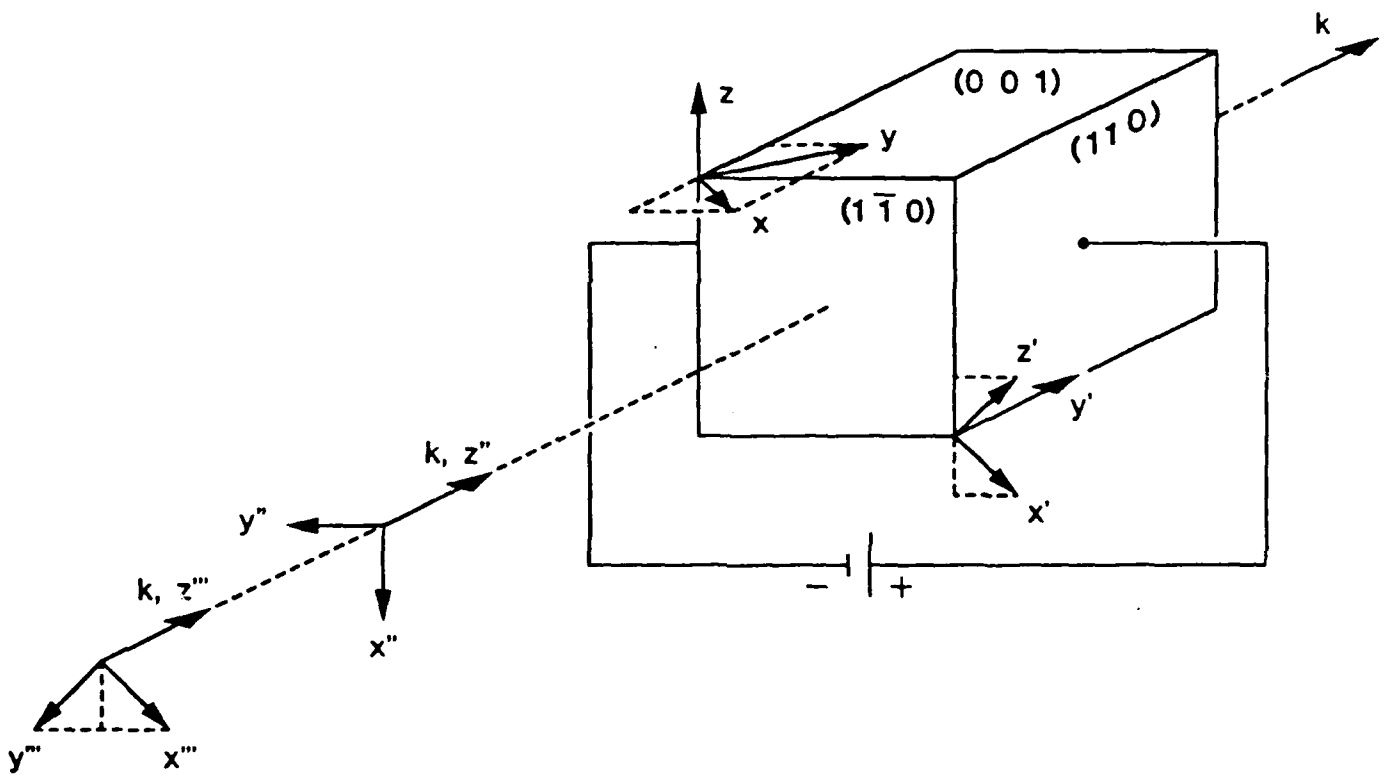


Fig. 9

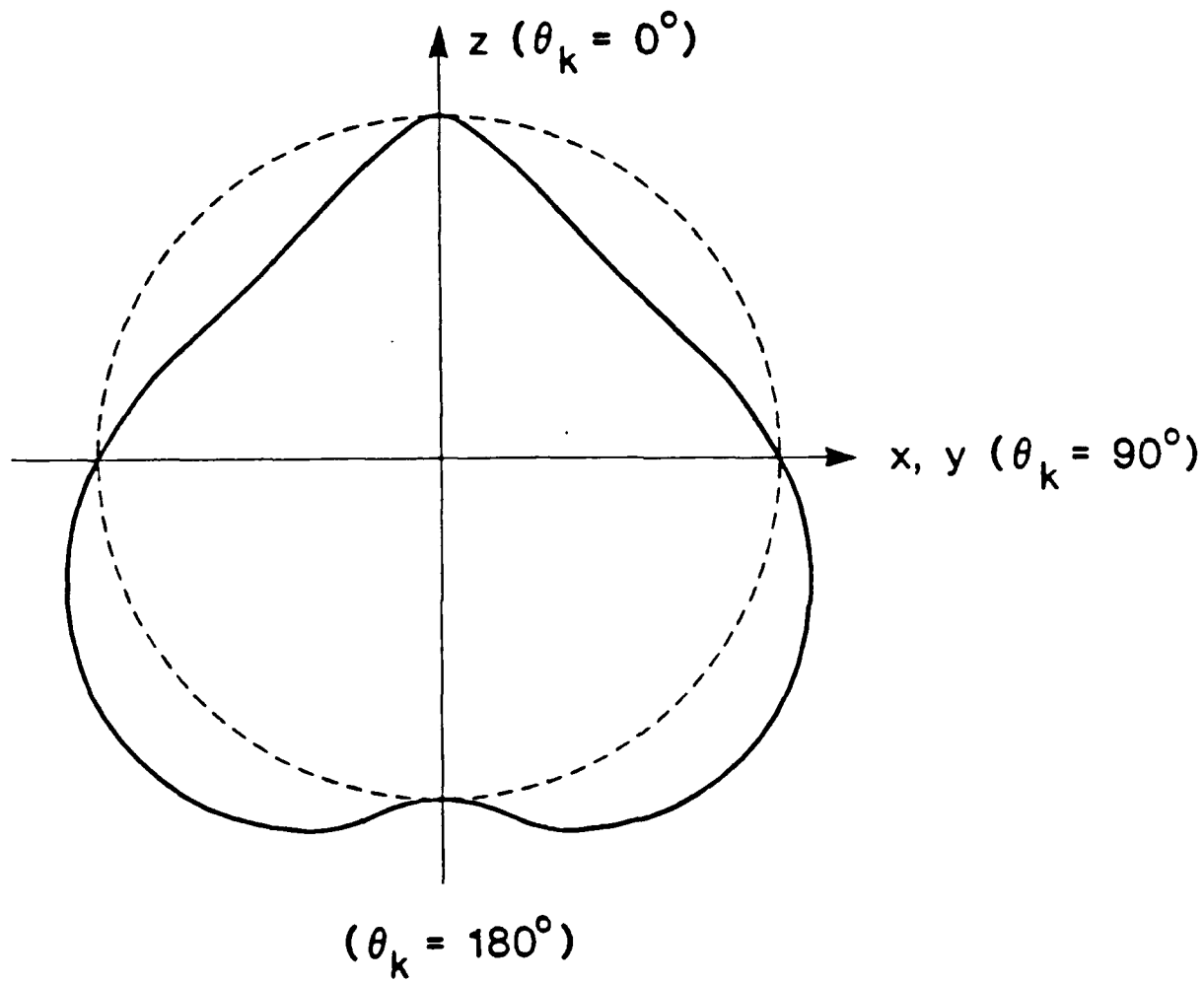


Fig.10